Impact of oxygen transfer dynamics on the performance of an aerobic granular sludge reactor

Strubbe, Laurence; van Dijk, Edward J.H.; Carrera, Paula; van Loosdrecht, Mark C.M.; Volcke, Eveline I.P.

DOI
10.1016/j.cej.2024.148843

Publication date
2024

Document Version
Final published version

Published in
Chemical Engineering Journal

Citation (APA)
Strubbe, L., van Dijk, E. J. H., Carrera, P., van Loosdrecht, M. C. M., & Volcke, E. I. P. (2024). Impact of oxygen transfer dynamics on the performance of an aerobic granular sludge reactor. *Chemical Engineering Journal*, *482*, Article 148843. https://doi.org/10.1016/j.cej.2024.148843

Chemical Engineering Journal 482 (2024) 148843

Contents lists available at ScienceDirect

Chemical Engineering Journal

journal homepage: www.elsevier.com/locate/cej

Impact of oxygen transfer dynamics on the performance of an aerobic granular sludge reactor

Laurence Strubbe [a], Edward J.H. van Dijk [b,c], Paula Carrera [a], Mark C.M. van Loosdrecht [c], Eveline I.P. Volcke [a,*]

[a] BioCo Research Group, Department of Green Chemistry and Technology, Ghent University, Coupure Links 653, 9000 Gent, Belgium
[b] Royal HaskoningDHV, Laan1914 35, Amersfoort 3800 AL, the Netherlands
[c] Department of Biotechnology, Delft University of Technology, Van der Maasweg 9, Delft 2629 HZ, the Netherlands

ARTICLE INFO

Keywords:
Oxygen transfer efficiency
Alpha factor
Simultaneous nitrification denitrification
aerobic granular sludge (AGS)
Modelling and simulation
Wastewater treatment

ABSTRACT

The aerobic granular sludge (AGS) process treats wastewater with a significantly lower footprint and energy consumption compared to conventional activated sludge systems. Nevertheless, there is still potential for optimizing its performance, and mathematical models are most valuable tools to this end. Aeration energy consumption deserves particular attention, as it is the largest remaining operating cost for AGS systems. Batch-wisely operated reactors show an increasing oxygen transfer efficiency during aeration, which translates into a dynamic alpha factor. However, the dynamic nature of alpha is neglected in current models. The impact of this simplification on the operating performance was addressed for the first time in this study. Through the development of a novel 1-D biofilm reactor model, calibrated to a full-scale AGS plant, it was shown that the alpha dynamics affect both model structure and calibration, as well as the process performance. The description of the dynamic nature of alpha through the empirical relationship with the soluble biodegradable organic carbon required the addition of the state variable representing soluble slowly biodegradable organic carbon (S_{CB}) to the biokinetic ASM2d model. Simulation results showed that alpha dynamics significantly influences simultaneous nitrification and denitrification and therefore need to be included in mathematical models to optimize AGS process performance. Different process variables such as volume exchange ratio, aeration capacity and granule size can be manipulated to improve reactor design and performance. The practical application of these new insights were discussed regarding the optimization of AGS systems, as well as other batch-wisely operated aerobic wastewater treatment systems.

1. Introduction

The aerobic granular sludge (AGS) technology has been widely recognized as a true innovation in the field of wastewater treatment due to its low footprint and energy use compared to conventional activated sludge systems. Nevertheless, there is still potential for optimizing its process performance [1] to keep a good effluent quality facing increasingly stringent standards and to further reduce the energy requirements. The lower pumping and mixing energy in batch-wisely operated AGS reactors compared to continuous activated sludge systems, results in a larger fraction of energy consumption dedicated to aeration (e.g. 67 % compared to 44 % for a Nereda® and Carrousel® systems respectively [2]). Optimizing aeration is crucial for both minimizing energy consumption and for maximizing treatment capacity.

The optimisation of aeration strategies for batch-wisely operated granular sludge reactors has been a topic of common interest [3–10]. Full-scale AGS batch reactors typically operate with continuous aeration at a fixed dissolved oxygen (DO) set-point. However, different studies have explored the potential benefits of adaptive process control, where the DO concentration is varied over the cycle to improve simultaneous nitrification and denitrification (SND) [4,5,11–13]. SND occurs when anoxic zones form within granules due to limited oxygen diffusion and the simultaneous diffusion and production of NO_3^- [14]. None of the studies investigating the optimisation of aeration strategies for batch-wisely operated granular sludge reactors has so far accounted for the dynamic nature of the alpha factor. The alpha factor defines the ratio of gas–liquid mass transfer in process water to clean water. It reflects the

* Corresponding author.
E-mail addresses: Laurence.Strubbe@UGent.be (L. Strubbe), edward.van.dijk@rhdhv.com (E.J.H. van Dijk), Paula.CarreraFernandez@UGent.be (P. Carrera), m.c.m.vanloosdrecht@tudelft.nl (M.C.M. van Loosdrecht), Eveline.Volcke@UGent.be (E.I.P. Volcke).

https://doi.org/10.1016/j.cej.2024.148843
Received 24 October 2023; Received in revised form 22 December 2023; Accepted 15 January 2024
Available online 18 January 2024

Nomenclature

Abbreviation	*Definition*
ANO	Autotrophic nitrifying organisms
ASM2d	Activated sludge model no.2d
COD	Chemical oxygen demand
DO	Dissolved oxygen
GAO	Glycogen accumulating organisms
N	Nitrogen
OHO	Ordinary heterotrophic organisms
P	Phosphorous
PAO	Phosphate accumulating organisms
PI	Proportional-integral controller
SBR	Sequencing batch reactor
SND	Simultaneous nitrification denitrification
VER	Volume exchange ratio
VFA	Volatile fatty acids
1-D	One-dimensional
Symbol	*Definition (Unit)*
$\bar{A}$	Average volume-weighted biomass surface area of the biomass fraction > 200 μm. (m^2)
$bCOD_S$	Soluble biodegradable organic carbon ($g.m^{-3}$)
$\bar{d}$	Average volume-weighted diameter (mm)
$d(i)$	Average diameter of size class i (mm)
$J_{Xi,bulk}$	Flux of particulate i in the boundary layer ($g.m^{-2}.d^{-1}$)
$k_La_{O_2,\,clean}$	Gas-liquid mass transfer coefficient of O_2 in clean water (d^{-1})
$k_La_{O_2}$	Gas-liquid mass transfer coefficient of O_2 in process water ($=\alpha F \bullet k_La_{O_2,\,clean}$) ($d^{-1}$)
MLSS	Total suspended solids in the mixed liquor (kg TSS. m^{-3})
$MLSS_g$	Total granular MLSS concentration (kg TSS. m^{-3})
$MLSS(i)$	MLSS concentration in size class i (kg TSS. m^{-3})
$MX_{i,bulk}$	Mass of particulate i (kg TSS)
n	Total number of size classes (-)
$n_g(i)$	Number of granules in size class i (-)
OTR	Oxygen transfer rate (kg $O_2.h^{-1}$)
OUR	Oxygen uptake rate (kg $O_2.h^{-1}$)
Q_{in}	Influent flow rate ($m^3.d^{-1}$)
Q_{out}	Discharge flow rate ($m^3.d^{-1}$)
$R_{i,bulk}$	Conversion rate in the bulk of particulate i ($g.m^{-3}.d^{-1}$)
S_F	Solute concentration of fermentables (readily biodegradable COD) ($g.m^{-3}$)
SRT	Sludge retention time (d)
S_{CB}	Solute concentration of slowly biodegradable COD ($g.m^{-3}$)
S_u	Solute concentration of inert COD ($g.m^{-3}$)
S_{VFA}	Solute concentration of volatile fatty acids (readily biodegradable COD)
ΔT_{cycle}	Total cycle length (h)
$\Delta T_{reaction}$	Reaction phase length (aeration + post-denitrification phase length) (h)
V_{bulk}	Bulk liquid volume (m^3)
V_g	Total granular biofilm volume (m^3)
$V_{reactor}$	Reactor volume (m^3)
X_i	Concentration of particulate i (kg $TSS.m^{-3}$)
$X_{TSS,bulk}$	Overall TSS concentration in the bulk liquid (kg $TSS.m^{-3}$)

Greek alphabet

αF	Alpha factor for fouled diffusers (-)
ρ_g	Biomass concentration in the granule (kg $TSS.m^{-3}$)
φ	Fraction of total bulk biomass wasted every cycle (-)
φ_i	Fraction of species-specific bulk biomass wasted every cycle (-)

Subscripts

bulk	In the bulk liquid
CB	Biodegradable
in	In the influent
PHA	Polyhydroxyalkanoate
PP	Poly phosphate
U	Unbiodegradable

low oxygen transfer efficiency at the start of the aeration phase in the batch operation due to operating and environmental conditions [15–17]. This can delay reaching the DO set-point, affecting the volume of aerobic and anoxic zones in the granule and consequently SND efficiency. As a result, the dynamic nature of the alpha factor may impact the treatment capacity of a batch-wisely operated AGS plant. Furthermore, a slow increase of the alpha factor over time may lead to an energy-inefficient operation. Therefore, this research hypothesises that neglecting the dynamic nature of the alpha factor in models could limit the accuracy and reliability of predicting treatment capacity, energy consumption, and process understanding.

Several algebraic correlations to describe the dynamic nature of alpha have been proposed for activated sludge with the aim to optimize the design and operation of aeration systems [18–25]. Three of these dynamic alpha models included a relationship between alpha and (influent) organic matter to address the short-term dynamics of alpha [20,21,25]. An exponential relation between alpha and the removal of soluble biodegradable COD ($bCOD_S$) was found for an AGS plant [15] similar to the empirical relation for activated sludge in batch operation proposed by [21]. Mathematical models applied to predict the performance of AGS systems, so far have focused on biokinetic processes, while only including a simplistic modelling of oxygen mass transfer [26].

The aim of this study was to investigate the impact of the dynamic nature of alpha on the performance of AGS batch reactors and to identify the shortcomings of current models that do not consider the dynamic nature of alpha. In this respect, a 1-D biofilm reactor model was developed and calibrated to a full-scale AGS plant to examine the difference in impact of a constant versus a dynamic alpha factor on the reactor performance. The AGS model with a case-specific dynamic alpha factor was made generally applicable by including the empirical relation between alpha and $bCOD_S$. This novel AGS model was used to assess alpha's impact on the performance of AGS reactors for different scenarios including a change in volume exchange ratio (VER, i.e., the ratio of the influent volume added to the total volume of the reactor), aeration capacity, temperature and granule size. Our previous study [15] demonstrated that the first three process variables influence the dynamic nature of the alpha factor. The granule size is hypothesized to also influence alpha dynamics as it determines the volume of aerobic and anoxic zones within the granule. Finally, the differences between the scenarios were analyzed to provide practical insights and perspectives to improve the optimization of AGS systems, as well as other batch-wisely operated aerobic wastewater treatment systems.

2. Material and methods

2.1. Reference case

The reference case for this study was the Prototype Nereda® in Utrecht, the Netherlands, of which the experimental data was used to calibrate the 1-D biofilm reactor model. This full-scale research installation is owned by the district water authority Hoogheemraadschap de

Stichtse Rijnlanden and is operated by Royal HaskoningDHV, who commercialized the AGS process under the trademark Nereda®. The reactor had a total volume of 1050 m^3, with a process water depth of 7.0 m and a surface area of 150 m^2.

Off-gas measurements were taken to analyse the dynamic behaviour of the alpha factor (αF) during the reaction phase of the batch cycle, as described in Strubbe et al. (2023). α F combines the effect of the alpha factor (α) and the fouling factor (F). Given that fouling is a slow phenomenon, it was reasonably assumed that F remained constant over the time period of the data analysis, so changes in αF could be attributed to changes in α.

The dataset that served as the basis for calibrating the model to the reference case consists of reactor, operating and biomass characteristics of an average batch cycle. The characteristics were determined by analyzing 14 batch cycles in the period 3–6 July 2020, during dry weather conditions. The material and methods related to the liquid phase measurements are specified in [15]. The average operating strategy included an anaerobic plug-flow feeding phase (1 h), an aeration phase (2.5 h), a post-denitrification phase (1.5 h), and a settling phase (0.5 h), resulting in an average total cycle length of 5.5 h. The applied VER was 25 %. During the aeration phase, the DO concentration was maintained at a constant set-point of 1 g $O_2.m^{-3}$. The gas–liquid mass transfer coefficient of O_2 in clean water, $k_La_{O_2,\,clean}$ (d^{-1}) determined according to the standard protocol DWA-M 209, 2007 of the German Association for Water, Wastewater and Waste is on average 148 d^{-1} at 20 °C [15]. The average operating temperature was 21.5 °C.

The biomass characteristics were based on data derived from a sample of the total suspended solids in the mixed liquor (MLSS) which was collected during the well-mixed aeration phase. Furthermore, the different size classes of the MLSS sample was determined by sieving the MLSS across a range of pore sizes (0.2, 0.63, 1.0, 1.4, and 2.0 mm) (Table S1). Based on this data, the volume-weighted mean diameter ($\bar{d}$ = 1.3 mm, Eq. S1), volume-weighted mean granular surface area ($\bar{A}$ = 1 200 000 m^2, Eq. S2) of the biomass fraction > 0.2 mm and the total granular biofilm volume (V_g = 160 m^3, Eq. S4) was calculated. Any solids smaller than 0.2 mm were classified as floccular biomass in this study. The reactor and operating characteristics are summarized in Table S2.

The reactor treated on average 1000 $m^3.d^{-1}$ with respective average influent concentrations of total organics, ammonium, and phosphate of 688 g COD·m^{-3}, 67 g NH_x-N·m^{-3}, and 5 g PO_4–P·m^{-3} during the reference period (Table S3). The influent COD was divided into soluble and particulate fractions, with the former including volatile fatty acids (VFA) ($S_{VFA,in}$), fermentable COD ($S_{F,in}$), and inert COD ($S_{u,in}$) and the latter consisting of biodegradable ($X_{CB,in}$) and inert ($X_{u,in}$) particulates based on the COD fractionation parameters determined by [27]. Further details regarding the influent concentrations are given in Table S3 and Fig. S1.

The model was calibrated to the reference case for the average concentration profiles of DO, NH_4^+ and PO_4^{3-} over the batch cycle during the reference period (Fig. S2). It took on average 1.6 h of aeration to reach the DO set-point of 1 g $O_2.m^{-3}$ for a continuous airflow rate of 800 $m^3.h^{-1}$ (Fig. S3), which is relatively long due to the limited aeration capacity (under dimensioning) of the reactor under study. The calibration of the DO profile between 0 and 1 g $O_2.m^{-3}$ has not been undertaken as such, given the different rates of increase observed in each aeration phase, which presents challenges for direct translation by the developed model. The NH_4^+ and PO_4^{3-} concentration profiles of this average batch cycle were reconstructed by calculating three average concentrations at specific time points: (i) at the start of the aeration phase, (ii) at 1 h of aeration, and (iii) at 1.5 and 2 h of aeration for PO_4^{3-} and NH_4^+ respectively. Concentration (i) was determined as the average measured concentration while concentration (ii) and (iii) were determined based on their average calculated maximal removal rate. This implies that the average concentration profile of PO_4^{3-} and NH_4^+, used for calibration, exhibits a decreasing linear trend, starting from the highest and approaching the lowest average measured concentration level (see calculation procedure in S.I. Section S.1.3.) During the subsequent post-denitrification phase, the PO_4^{3-} and NH_4^+ concentrations remain relatively stable, around the detection limits of 0.05 mg $P.L^{-1}$ and 1 mg $N.L^{-1}$ (Fig. S2).The average maximal removal rates for NH_4^+ and PO_4^{3-} were determined as 3.6 mg $N.L^{-1}.h^{-1}$ and 6.7 mg $P.L^{-1}.h^{-1}$, respectively. On average, 20 % of the removed NH_4^+ is adsorbed to the biomass at the start of the aeration phase [28], so the NH_4^+ consumption rate was estimated to be 4.5 mg $N.L^{-1}.h^{-1}$. The calculated NH_4^+ consumption rate and PO_4^{3-} uptake rate were compared to values reported by [1] (i.e. 2.4 and 7 mg $N.L^{-1}.h^{-1}$ and 0.45 and 10 mg $P.L^{-1}.h^{-1}$, respectively) and found to be representative of a full-scale AGS batch reactor. The measured NO_3^- concentrations were unsuitable for calibration since they consistently fell within the range of 0.5–3.5 mg $N.L^{-1}$, posing a challenge for qualitative interpretation given the accuracy of 0.5 mg $N.L^{-1}$.

2.2. One-dimensional biofilm reactor model

The behaviour of the AGS reactor was described with a one-dimensional (1-D) biofilm reactor model. Whereas most previous studies used the Aquasim [29] simulation environment [30], the 1-D AGS reactor model in this study was implemented in Matlab-Simulink (The Math Works, Inc. MATLAB. Version R2020a) to allow more easy and flexible testing of operating strategies. The model consists of (1) a bulk compartment, (2) a biofilm compartment, and (3) bioconversions (Fig. 1).

2.2.1. Bulk compartment

The bulk compartment simulates the batch operation of the AGS reactor under study, assuming completely mixed conditions in each phase of the cycle. In reality, completely mixed conditions do not apply during the anaerobic simultaneous feeding and discharge phase of the batch operation, which was taking into account through the following four model modifications. First, the high concentration gradients during anaerobic plug flow feeding were mimicked by increasing the value of the diffusion coefficient of acetate by a factor five [31]. The diffusion coefficient of other soluble biodegradable organic carbons was held constant as they did not exert a rate-limiting effect on the observed concentration profiles during anaerobic feeding. Secondly, the bioconversion reactions in the floccular biomass were turned off to mimic selective feeding of granules over flocs. Flocs are typically situated on top of the sludge bed, resulting in a minimal supply of feed left for the flocs [32]. Thirdly, denitrification and inhibition of NO_3^- were excluded during the feeding period. In practice, the plug-flow regime causes the accumulation of NO_3^- from the previous cycle at the upper part of the reactor, while the granular sludge bed experiences anaerobic conditions. Lastly, to ensure a correct removed water volume and fulfil the correct VER during the anaerobic feeding phase, a separate discharge phase of negligible duration (5 min) was included. These four corrections made sure that PAOs were selected over OHOs in the granular biomass which was important to correctly predict the total phosphorous effluent quality [11]. Fig. S6 visually compares the actual and modelled batch operation. A proportional-integral (PI) controller with anti-windup was used for the oxygen control strategy, with controller parameters listed in Table S9.

The model considered an average fixed floccular biomass concentration ($X_{TSS,bulk}$) of 1.5 kg TSS.m^{-3} in the bulk based on experimental data (Table S1, $X_{TSS,bulk} = X_{U,bulk} + XC_{B,bulk} + X_{OHO,bulk} + X_{PAO,bulk} + X_{ANO,bulk}$, in kg TSS.$m^{-3}$). To maintain the fixed biomass concentration, only a fraction of the floc concentration was wasted every cycle. The factor φ represented this fraction and had the same value for every particulate in the mass balance [33]. However, later in this study it was found necessary to include a species-specific wasting factor, φ_i, the value of which was different for each type of particulate (see further). The mass balance of a specific particulate over time is given by Eq. S17.

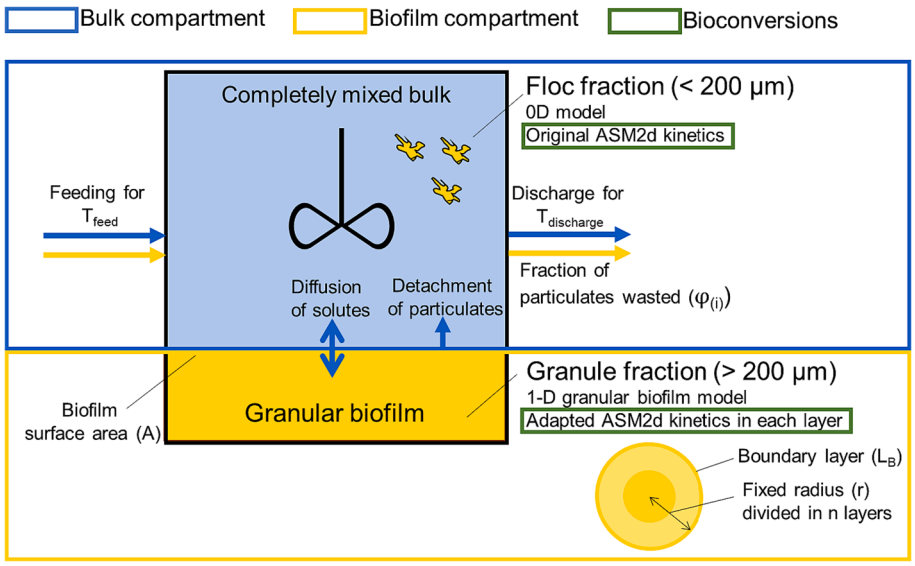

Fig. 1. Schematic representation of the 1-D biofilm reactor model features developed in this study.

2.2.2. *Biofilm compartment*

The dynamic concentration gradients of solutes and particulates within the granules were described by the 1-D biofilm model developed by [33,34]. The granules were assumed to have a fixed size which was achieved to set detachment rates equal to the growth rates. To balance numerical accuracy and efficiency, each granule was subdivided into 25 layers, each 0.03 mm thick, which is comparable to the size of an activated sludge floc [35]. The detachment of particulates from the granules contributes to the floccular biomass in the bulk, impacting the bulk liquid species composition and solid retention time (SRT) per species. The model was implemented in MATLAB-Simulink® R2020a software. Detailed information on the biofilm model can be found in S.I. section S2.2.

2.2.3. *Bioconversions*

The biokinetic model used in this study was ASM2d [36], corrected on typos by [37]). In this model, OHO and PAO are responsible for COD removal and denitrification, with the PAO also performing P uptake and the ANO performing nitrification. In this study, phosphorus precipitation, redissolution reactions and alkalinity were not considered (omitted from ASM2d). Furthermore, incorporation of P in the biomass was not included in the stoichiometry and kinetics to minimize computational errors [9].

The ASM2d kinetic parameters were applied except for the decay rates of PAO which were decreased from 0.2 to 0.02 d^{-1} as in [9] in order to account for the protective effects of the granule structure and EPS layers [38]. Detailed information on the bioconversions can be found in S.I. section S2.3.

2.3. *Research approach*

In this work, the model development and calibration to the reference case at steady-state conditions was carried out in three steps: (1) a constant maximum alpha ($\alpha F = 1$), (2) a time-dependent alpha ($\alpha F = \alpha F(t)$), and (3) an alpha dependent on the removal of $bCOD_S$ ($\alpha F = \alpha F(bCOD_S(t))$). The first two steps were compared to investigate whether the dynamic nature of alpha does have a significant impact on the process performance of an AGS reactor. The addition of the empirical relation between alpha and $bCOD_S$ in the third step was necessary to assess the impact of the dynamic nature of the alpha factor on process performance for different design and operating strategies, which was investigated as the fourth step of the research approach followed in this work. The quality of the model calibration was evaluated through the minimal sum of squared errors between the measured and simulated concentrations Fig. S11 visualizes the four steps of the research approach.

2.3.1. *Step 1: Constant (ideal) alpha*

The 1-D biofilm reactor model was calibrated by adjusting its parameters to reflect the bulk MLSS concentration and the concentration profiles of NH_4^+ and PO_4^{3-} during the batch cycle of the reference case. This calibration was performed under constant average operating and influent conditions. The model assumed a constant maximum alpha factor of 1, which means that the gas–liquid mass transfer coefficient in process water was assumed equal to the one for clean water ($k_La_{O_2} = \alpha F \bullet k_La_{O_2,\,clean} = 148\ d^{-1}$ as determined in [15]). The MLSS concentration in the bulk liquid was determined by a wasting factor φ with the same value for all microbial species.

2.3.2. *Step 2: Time-dependency of alpha*

A time-dependent alpha factor $\alpha F = \alpha F(t)$, increasing from $\alpha F = 0.25$ at the start of aeration to a maximum value of $\alpha F = 0.55$, was incorporated in the model according to the first-order relation determined by Strubbe et al. (2023) [15], on experimental data of the same reference case as applied in this study (see S.I. section S3.2). The resulting model was again calibrated to the reference case. The oxygen uptake rate (OUR, kg $O_2.h^{-1}$) for different species (OHO, PAO, and ANO) was compared to the oxygen transfer rate (OTR, kg $O_2.h^{-1}$) for both step 1 and 2. Details about the calculation methods can be found in S.I. section S3.2.

2.3.3. *Step 3: Dependency of alpha on concentration of soluble biodegradable organic carbon*

The dependency of the alpha factor on the soluble biodegradable organic carbon $\alpha F = \alpha F(bCOD_S(t))$ has been postulated to be the explanation for its time-dependent behaviour [15]. Therefore, in order to describe the dynamic behaviour of the alpha factor in a more general way, which can also be applied to different design and operating strategies, the empirical relation between alpha and $bCOD_S$ from Strubbe et al. (2023) was used, as shown in Fig. S13.

The alpha factor is affected by both readily and slowly soluble biodegradable organic carbon [15]. However, the ASM2d model assumes all soluble biodegradable organic carbon to be readily biodegradable, while particulate organic carbon components are considered slowly biodegradable [36]. This assumption is not entirely accurate as some colloidal organic fractions can be measured as soluble, even

though they are slowly biodegradable [39]. To address this issue, the biokinetic ASM2d model was modified by dividing the soluble components into a readily biodegradable fraction (S_{VFA} + S_F), and a slowly degradable fraction (S_{CB}), as done by [40] for a high-rate activated sludge process. The reactions of the different biodegradable COD components, either particulates or solutes, over the different batch phases, of the extended ASM2d model are visualized in Fig. 2. The model was calibrated by adjusting the fractionation of solutes into S_F and S_{CB} (Fig. S1), as well as the biokinetic parameters of S_{CB}. The extension of the ASM2d model can be found in S.I. section S2.3.

2.3.4. Step 4: Scenario analysis

The 1-D biofilm reactor model calibrated to the reference case, with alpha dependent on $bCOD_S$ concentration over the aeration phase, was used to assess the impact of alpha on the performance of AGS reactors for different scenarios, including a change in (i) VER, (ii) aeration capacity (related to $k_La_{O_2,\,clean}$), (iii) average granule size and (iv) temperature. The feeding, discharge, and settling times remained constant in comparison to the reference case, but the length of the reaction phase, which includes both the aeration and post-denitrification phase lengths, varied. More specifically, the aeration phase was switched off when NH_4^+ reached a concentration of 3 mg NH_4^+-N.L^{-1} while the length of the post-denitrification phase was determined by an end concentration of 3 mg NO_3^--N.L^{-1}. The performance of each scenario was analysed in terms of treatment capacity (m^3.d^{-1}), SND efficiency (%), and oxygen transfer efficiency (OTE, %) (related to energy consumption). The process performance was considered optimal when achieving the desired effluent quality while maximizing the treatment capacity and minimizing energy consumption. Details of the model adaptations per scenario and calculation methods can be found in S.I. section S3.4.

3. Results and discussion

3.1. Effect of alpha dynamics on reactor performance

The 1-D biofilm reactor model was calibrated to the reference case for both a constant maximum alpha = 1 and a time-dependent alpha factor (Fig. 3b and e respectively). The implications of assuming a constant maximum alpha versus considering the dynamic nature of alpha are discussed in view of the model structure, calibration and predicted reactor performance, i.e. the treatment capacity and energy consumption.

3.1.1. Effect of alpha on model structure and calibration

The calibration approach varied significantly between the model assuming a maximum alpha compared to the model considering the observed time-dependent dynamic behaviour of alpha. When a maximum alpha factor was used, the oxygen transfer efficiency and thus oxygenation capacity of the system was overestimated. More specifically, the model with dynamic alpha predicts a 33 % lower oxygen transfer efficiency compared to the model with a constant maximum alpha (Eq. S37, the difference in $k_La_{O_2}$ is indicated by the red area in Fig. 3d). The lower oxygen transfer efficiency resulted in a better match with the average time (1.6 h) to reach the DO set-point of 1 g O_2.m^{-3}, thereby validating the model with dynamic alpha in its more accurate prediction of the system's oxygenation capacity compared to a model with a constant maximum alpha.

The overestimation of the oxygenation capacity for the model with a constant maximum alpha of 1 caused faster phosphate uptake and nitrification compared to the experimental data before calibration (Fig. S14). Model calibration, which was performed in three steps, allowed to match the simulated concentration profiles with the experimentally determined bulk MLSS concentration and NH_4^+ and PO_4^{3-} profiles. First, the bulk MLSS concentration of 1.5 kg TSS.m^{-3} was calibrated by estimating the parameter φ, which represents the fraction of total bulk particulates (X_{TSS}, kg TSS.m^{-3}) wasted every cycle (Eq. S17). Through the process of trial and error, φ was set at 0.2, meaning that 20 % of X_{TSS} was wasted every cycle. Secondly, the NH_4^+ concentration profile over the aeration phase was calibrated by decreasing the calculated total granular biofilm surface area, $\bar{A}$, per 100 000 m^2 until NH_4^+ concentration profile matched the measured values (Fig. 3b). The rate of decrease in NH_4^+ concentration was judged to be adequately simulated and did not need further calibration. Finally, the PO_4^{3-} concentration profile over the aeration phase was calibrated by adapting five kinetic parameters related to the PAO metabolism to correctly simulate the end of phosphate uptake as determined experimentally (Fig. 3b). Note that GAO activity was not modelled explicitly due to the limited added insights related to the impact of alpha on the process performance. Neglecting GAO activity led to a higher simulated phosphate release compared to practice, as all VFA was assumed to be stored only by PAOs. The calibrated model parameters for a constant alpha are summarized in Table 1..

The calibration approach for the model with a dynamic alpha factor exposed a limitation in the 1-D biofilm reactor model. The low oxygenation capacity of the system limited the ANO population in the granules. Moreover, the model assumed that granules had a fixed size and that growth products were detached in the bulk phase. Consequently, the simulated biomass population in the bulk phase largely reflected the simulated biomass population in the granules, causing an underestimation of the SRT of the floc fraction (Eq. S39). Due to the limited oxygenation capacity of the system, it is assumed that the ANO population lives in the smaller granular fraction or the so-called floc fraction. However, the wasting factor φ (0.2) reduced the SRT of the floc fraction to less than 5 days. As a result, the model was unable to accurately predict the experimentally determined nitrification capacity. To address this issue, a species-specific wasting factor φ_i was introduced in the model, allowing to capture the SRT distribution for different size classes in an AGS reactor. The AGS process is engineered to selectively waste the poor settling biomass while retaining the best settling granules. Consequently, an SRT distribution exists across the different

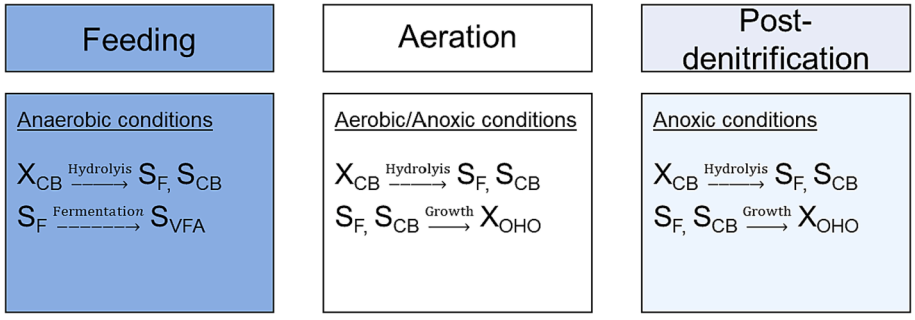

Fig. 2. Visualization of the different biodegradable COD components, either particulates (X) or solutes (S), over the different batch phases, of the extended ASM2d model.

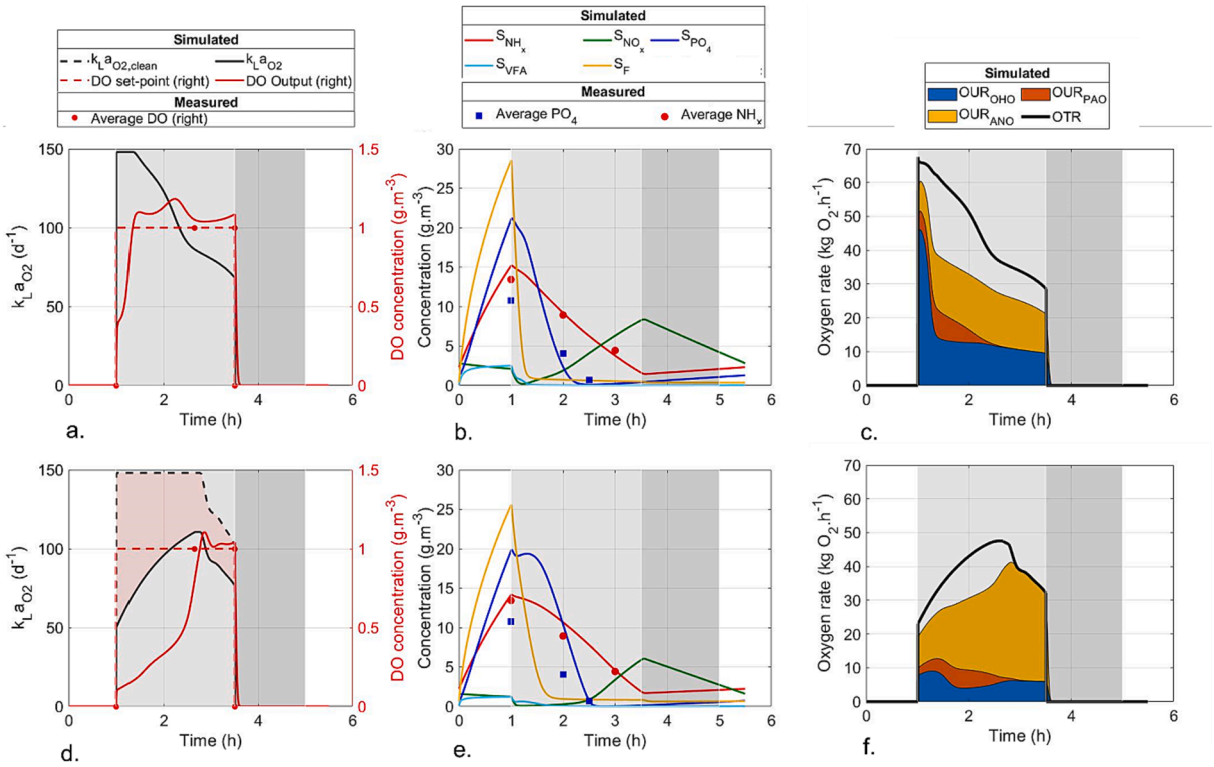

Fig. 3. Simulation results of the model calibration at steady state with the average measured values of 14 batch cycles between 3 and 6 July 2020 of the reference case for a constant maximum alpha = 1 (top graphs, a-c) and a time-dependent alpha factor (bottom graphs, d-f). (a) and (d): simulated DO set-point ($g.m^{-3}$), PI controller's manipulated $k_La_{O_{2,clean}}$, and the effective$k_La_{O_2} = \alpha F \bullet k_La_{O_{2,clean}}$ (d^{-1}), controlled and measured DO concentration ($g.m^{-3}$). b and e: simulated and measured concentration profiles ($g.m^{-3}$). c and f: oxygen uptake rate (OUR, kg $O_2.h^{-1}$) for different species (OHO, PAO, and ANO) compared to the oxygen transfer rate (OTR, kg $O_2.h^{-1}$). The light grey shaded area represents the aeration phase, whereas the dark grey shaded area denotes the post-denitrification phase.

Table 1
Original values of the biokinetic (ASM2d [36]) and reactor model parameters compared to the calibrated parameters for the model with a constant maximum alpha (αF = 1), with a time-dependent alpha, αF(t), and alpha dependent on the biodegradable soluble organics, αF($bCOD_S$).

Symbol	Definition	Original value	Calibrated value for αF = 1	Calibrated value for αF(t)	Calibrated value for αF($bCOD_S$)	Unit
Influent characteristics						
S_F	Fermentable organic matter	200	200	200	180	g COD.m^{-3}
S_{CB}	Slowly biodegradable soluble organic matter	n.a.	n.a.	n.a.	20	g COD.m^{-3}
Reactor and biomass model parameters						
φ	Fraction of total bulk biomass wasted every cycle	n.a.	0.2	n.a.	n.a.	–
φ_U	Fraction of unbiodegradable particulate organics wasted every cycle	n.a.	n.a.	0.6	0.6	–
$\varphi_{CB,\ OHO,\ PAO,\ PP,\ PHA}$	Fraction of biodegradable particulate organics, heterotrophic organisms and storage polymers wasted every cycle	n.a.	n.a.	0.4	0.4	–
φ_{ANO}	Fraction of autrophic nitrifying organisms wasted every cycle	n.a.	n.a.	0.04	0.04	–
A	Total granular biomass surface area	1 200 000	800 000	1 200 000	1 200 000	m^2
C	Correction factor for αF	1	1	1.35	1.35	–
Biokinetic model parameters						
b_{PAO}	Decay rate of X_{PAO}	0.02*	0.05	0.02	0.02	d^{-1}
$b_{PP\_PO_4}$	Rate constant for lysis of $X_{PAO,PP}$	0.02*	0.05	0.02	0.02	d^{-1}
b_{Stor_VFA}	Rate constant for respiration of $X_{PAO,Stor}$	0.02*	0.05	0.02	0.02	d^{-1}
$q_{PAO.PO_4\_PP}$	Rate constant for storage of $X_{PAO,PP}$	1.5	1	1	1	g P.(g COD)$^{-1}$.d^{-1}
$f_{PP\_PAO,Max}$	Maximum ratio of $X_{PAO,PP}/X_{PAO}$	0.34	0.204	0.204	0.204	g P.(g COD)$^{-1}$

*Values given by [9] were assumed to be the original ones applicable for an AGS system as a value of 0.2 d^{-1} [36] eliminates any PAO activity in the system.

granule sizes. The calibration approach in this case was iterative. First, the wasting factor of the inert particulates, φ_U, was adapted to match the experimentally determined MLSS concentration in the bulk of 1.5 kg TSS.m^{-3}. Secondly, the total granular biofilm surface area, $\bar{A}$, was again set to the calculated value to improve the growth of ANOs in the granules. The wasting factor of ANOs, φ_{ANO}, was decreased while the

wasting factor of the other organisms and biodegradable particulates ($\varphi_{CB, OHO, PAO, PP, PHA}$) and was increased compared to the general φ of 0.2. It increased the SRT of ANOs and lowered the oxygen consumption respectively. Thirdly, the decay rate of PAOs was again reduced to fit the end of phosphate uptake rate (Fig. 3e). Finally, the increase in alpha was corrected to calibrate the average time to reach the DO set-point of 1 g $O_2.m^{-3}$ (Fig. 3d). The calibrated model parameters for the time-dependent alpha factor are given in Table 1. Note that simulations for a constant minimum, maximum and average alpha factor were conducted as well (Fig. S16). Explicitly incorporating alpha dynamics was determined to be the most suitable approach, since their effect on the removal rates deviated significantly from the more realistic dynamic alpha behaviour.

3.1.2. Effect of alpha on the treatment capacity and energy consumption

While optimising the AGS process, a constant maximum alpha is often considered through the assumption that the DO set-point is reached instantaneously [3,4,9,11,31,41–43]. However, this research has shown that a dynamic alpha not only affects the model structure and calibration, but also the process performance, i.e. treatment capacity and energy consumption.

The difference between a constant maximum and dynamic alpha factor resulted in a different distribution of ANOs over the granule and floc fraction. In case of the maximum alpha, the ANOs were evenly distributed over both fractions (Fig. S17). However, with a dynamic alpha, a larger proportion of ANOs were present in the floc fraction (Fig. S18). This has been supported by several studies, along with full-scale measurements [44], which have shown that in smaller granules nitrifying organisms are enriched due to a larger relative aerobic volume [45,46]. This variation in ANO distribution between the two cases was reflected in the simulated oxygen uptake rate (OUR) profiles. In the case of a constant maximum alpha, the OUR declined over time, in line with substrate concentrations. However, in case of a dynamic alpha, the OUR of ANOs increased during the aeration period. Initially, during the oxygenation capacity-limited phase, the OUR of PAO and OHO was at its maximum. As their activity decreased and the oxygenation capacity diminished, oxygen reached the ANO population in the granules as well, stimulating their activity and increasing their OUR.

The difference in ANO distribution and OUR profiles was also reflected in the model predictions of SND efficiency (reflected by the difference in NH_4^+ and NO_3^- peak), where the dynamic alpha resulted in a higher SND efficiency (52 %) compared to the maximum alpha (39 %). The higher SND efficiency is in line with historical data of the plant under study (data not shown) and the measured NO_3^- concentration at the end of aeration (i.e. 0.5–3.5 mg $N.L^{-1}$, with an accuracy of 0.5 mg $N.L^{-1}$). Therefore, the hypothesis is that incorporating the dynamics of alpha into the model leads to a better estimation of changes in OUR over time (Fig. 3f). This, in turn, enabled more accurate predictions of SND efficiency (Fig. 3e) and thus treatment capacity. The reported efficiencies of AGS treating municipal wastewater (SND) vary greatly, ranging from 70 % to 10 % (Fig. 1, Layer et al. (2020)). This simulation highlighted that electron-donor availability is not the sole influencing factor on SND efficiency, contrary to the conclusions of Layer et al. (2020). The dynamic alpha factor should also be considered. Besides, considering the dynamic nature of alpha gave a more realistic prediction of the oxygen transfer efficiency (Fig. 3d) and thus the related energy consumption.

3.1.3. Reference case with alpha dependent on the concentration of biodegradable organics

To evaluate the impact of the alpha factor on process performance for different operating strategies, the empirical relation between alpha and the $bCOD_S$ concentration over the aeration phase length replaced the time-dependent relation of alpha. The simulated $k_La_{O_2}$ for both cases, along with the different $bCOD_S$ concentrations over time, are shown in Fig. 4. The $k_La_{O_2}$ profiles were in good agreement with each other, demonstrating the success of the calibration. The nutrient concentration profiles and OUR over time are not shown, but were found to be similar to those of the time-dependent alpha case (Fig. 3e and f). The calibrated model parameters for the alpha factor dependent on $bCOD_S$ are given in Table 1.

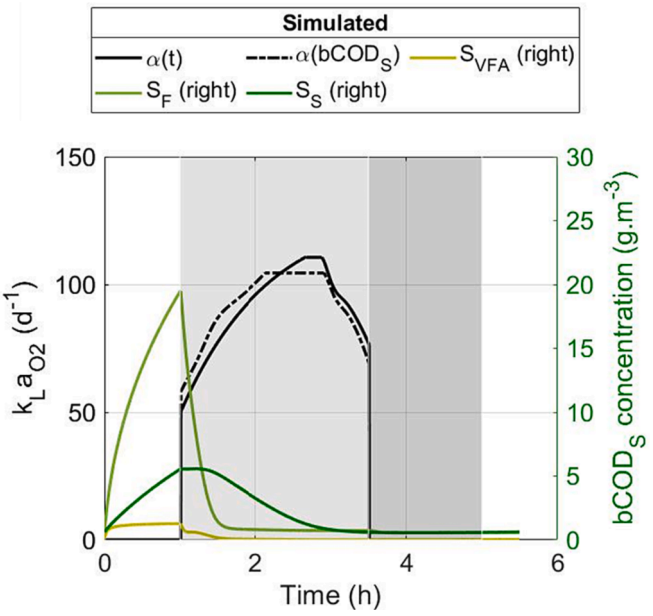

Fig. 4. Simulated oxygen mass transfer coefficient ($k_La_{O2} = \alpha F \bullet k_La_{O_{2,clean}}$, d^{-1}) for the alpha factor described by the time-dependent first-order relation ($\alpha F(t)$) compared to the alpha factor related to the soluble biodegradable organic carbon ($\alpha F(bCOD_S)$) determined by [15]. $bCOD_S$ is defined as the sum of readily $S_{VFA}(t)$, $S_F(t)$ and slowly biodegradable COD $S_{CB}(t)$ of which the concentration profiles are shown on the right y-axes.

The dynamic aeration model, which takes into account the relationship between alpha and the bCODS concentration over the aeration phase length, was integrated for the first time in an AGS model which allows to simulate how alpha dynamics impact process performance. The calibrated AGS model with the dynamic aeration model can now be used for scenario analysis.

3.2. Scenario analysis

3.2.1. Influence of volume exchange ratio

When taking into account alpha dynamics, an operating optimum in VER exist (Fig. 5a). A VER of 25 % increased the treatment capacity by 13 % compared to a lower VER of 12.5 %, while a VER of 50 % was 7 % lower compared to the VER of 25 %. This is explained by the fact that a low VER resulted in a fast alpha increase due to low $bCOD_S$ concentrations at the start of the aeration phase, resulting in a shorter reaction time. However, the total treatment capacity (Eq. S35) was reduced because the feeding and settling times remain the same, regardless of the shorter aeration time, resulting in a longer cycle time per volume of wastewater treated. Conversely, a high VER led to a slow alpha increase and thus a low oxygen transfer efficiency, which was particularly pronounced at the start of the aeration. This low oxygen transfer efficiency, led to a prolonged period of limited oxygenation capacity, which in turn, slowed down all conversion rates, further extending the 'alpha-delay'. Moreover, the limited oxygenation capacity caused a delay in nitrification, leading to a decrease in SND efficiency of 10 % (Fig. 5b). In the end, the higher VER of 50 % led to a disproportionately longer reaction phase compared to a lower VER of 25 %, which eventually decreased the treatment capacity. However, when considering energy consumption, a lower VER was the most beneficial option, as it was associated with the highest oxygen transfer efficiency (Fig. 5c).

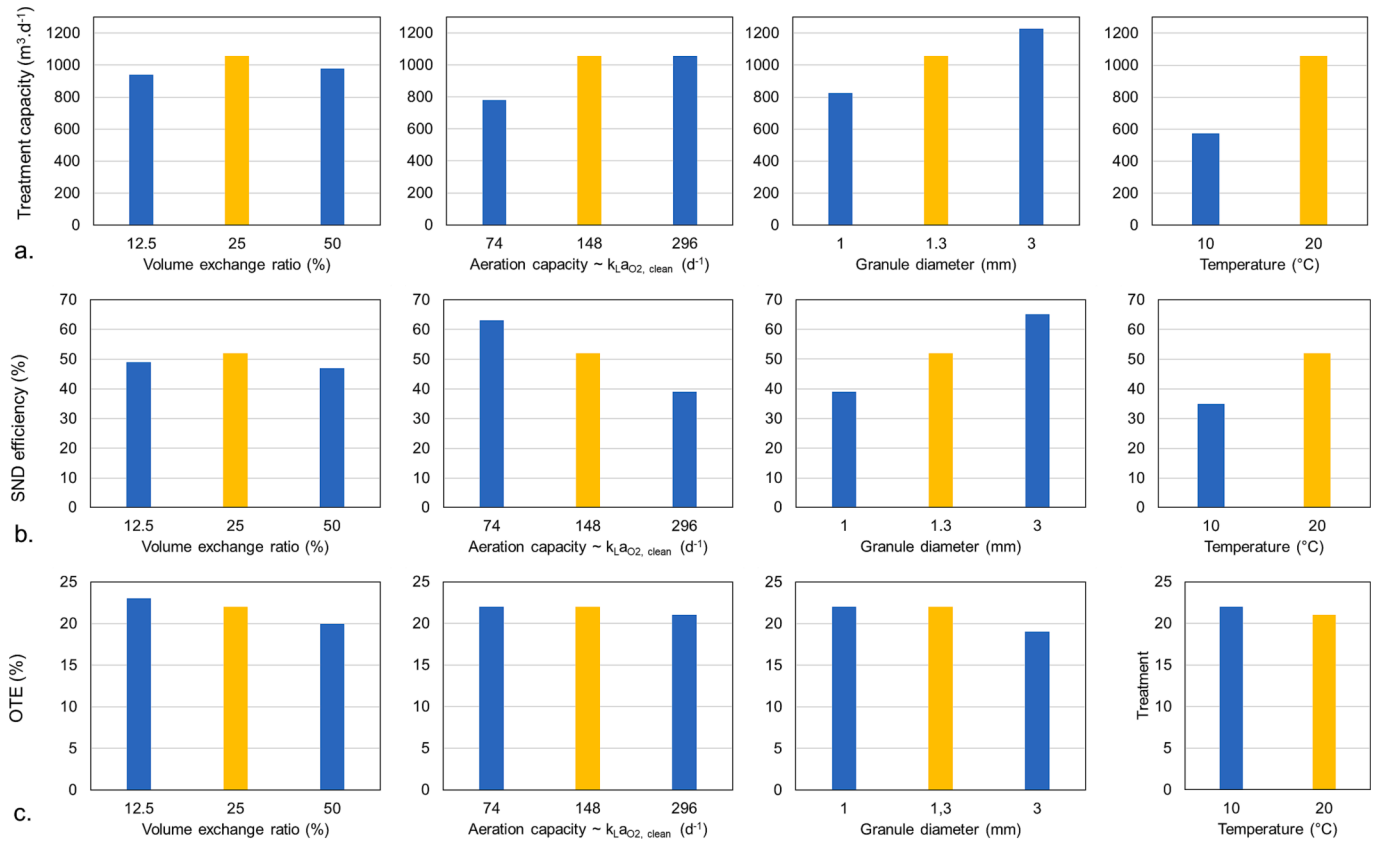

Fig. 5. Overview of the different scenarios with dynamic alpha factor and their effect on (a) the treatment capacity ($m^3.d^{-1}$), (b) simultaneous nitrification and denitrification (SND) efficiency (%) and (c) the oxygen transfer efficiency (OTE, %). The reference case is marked in yellow.

In practice, the VER is often determined by the incoming wastewater flow rate, the selected cycle time and other boundary conditions, e.g. respecting a maximum practical VER of 65 % and keeping a maximum liquid upflow velocity of 5 $m.h^{-1}$ [47]. Moreover, the pollutant load and the consequent increase in alpha cannot be solely attributed to the VER, as assumed in this study, since the wastewater strength is highly dynamic due to daily activity and weather conditions. The optimal VER and cycle time to be applied in practice should consider all of these effects. Additionally, although the differences in oxygen transfer efficiency were not significant (Fig. 5c), they do provide insight into potential influences on energy efficiency. However, it will be important to validate its impact on energy consumption at full-scale plants.

3.2.2. *Influence of aeration capacity*

When taking into account alpha dynamics, an optimum in installed aeration capacity exist (Fig. 5a). Halving the aeration capacity (74 versus 148 d^{-1}) resulted in a lower system's oxygenation capacity, which led to slower conversion rates, lengthening aeration times, and thus a 26 % lower treatment capacity. However, doubling the aeration capacity (296 versus 148 d^{-1}) reduced the SND efficiency, resulting in a disproportionately longer post-denitrification phase. This was caused by a higher DO concentration at the start of the aeration phase, which decreased the SND efficiency (Fig. 5b). Despite a decrease in the aeration phase length, the post-denitrification phase length increased, resulting in the same overall reaction phase length as the reference case. Consequently, a higher aeration capacity did not improve the treatment capacity of the system (1056 $m^3.d^{-1}$ for both cases). While increasing the aeration capacity led to a faster achievement of the DO set-point and improved the oxygen transfer, it did not result in improved aeration efficiency, which remained constant for all cases (Fig. 5c). In fact, the higher aeration capacity consumed more oxygen compared to the lower capacity, as more COD was oxidized aerobically instead of being utilized through SND. Consequently, despite the higher mass flow of oxygen supplied by the blower to the aeration tank, a larger mass of oxygen was consumed, resulting in the same average oxygen transfer efficiency. This offsets any potential gain in energy efficiency that may have arisen from a faster increase in alpha. Note that this scenario of a larger aeration capacity aligns with an aeration strategy in which extra aeration capacity at the start of the aeration phase is used, enabling the rapid achievement of the DO set-point. However further research could investigate an optimal aeration strategy which optimizes the OTE, while still ensuring enough capacity for SND, e.g. through the use of 2-step or alternating aeration [4].

In practice, it is more economically advantageous to install a lower aeration capacity. Moreover, it is important to consider that the available surface area in the reactor design can limit the installed aeration capacity, which may restrict the options for system optimization. Neglecting the blower's optimal working area may further constrain system optimization [48]. The aeration capacity needs to be optimized within the constraints of available surface area and achieve a balance between installation costs, blower efficiency and treatment capacity.

3.2.3. *Influence of granule size*

When taking into account alpha dynamics, an optimum in granule size exist (Fig. 5a). Larger granules have a lower specific surface area, which makes them more diffusion limited, compared to smaller granules. However, diffusion limitation of oxygen enhanced SND efficiency for larger granules, as shown in Fig. 5b. This resulted in a shorter post-denitrification phase length, which, in turn, increased treatment capacity (Fig. 5a). Despite this, a larger average granule size resulted in a decreased oxygen transfer efficiency (Fig. 5c) due to their mass transfer limitations of COD and lower uptake of VFA during the anaerobic feeding phase. This led to a higher $bCOD_S$ concentration at the start of the aeration phase, resulting in a slower increase of alpha and thus a

lower oxygen transfer efficiency. Therefore, it is necessary to achieve an optimal balance between treatment capacity and oxygen transfer efficiency.

Contrary to expectations, the simulation results did not show an improvement in the aeration phase length with smaller granules, despite the higher biofilm surface area. In fact, the model showed a decrease in OHO bulk concentration due to the lower $bCOD_S$ concentration at the start of the aeration phase (Fig. S18). Consequently, there was an accumulation of particulate COD in the bulk, leading to a lower SRT of ANOs, decreasing the nitrification rate. Furthermore, due to the lower SND efficiency of smaller granules, a longer post-denitrification phase length is required, further decreasing the treatment capacity (Fig. 5a).

The effect of granule size on SND has been extensively studied [4,14,46,49,50]. However, it remains challenging to control granule size in practice due to the various mechanisms influencing granulation [32]. Furthermore, there is a poor correlation between average granule size and nitrification capacity because it depends on individual size fractions and their distribution in ANOs [45]. A uniform average granule size may not equate to the same SND capacity due to differences in granule size distribution. Investigating the incorporation of granule size selection in full-scale reactor operations to enhance SND is worthwhile.

3.2.4. Influence of temperature

Temperature can have contrasting effects on bioconversion rates and oxygen transfer efficiency. While a lower temperature decreased bioconversion rates, it increased the oxygen saturation concentration, thus increasing the oxygenation capacity of the system. With more oxygen available, conversion rates were improved despite the lower temperature, accelerating the increase of alpha. However, the model simulations showed that lower conversion rates still prevailed and ultimately decreased the treatment capacity and SND efficiency (Fig. 5a an b respectively). From an energy perspective, the aeration efficiency was not negatively impacted by the lower conversion rates at lower temperatures because the increased oxygen transfer compensated for the reduction in bioconversion rates (Fig. 5c).

De Kreuk et al. (2005) [51] recommended to control the DO concentration in the reactor to ensure optimal effluent quality across different seasons. However, our research also highlighted the importance of considering the dynamic alpha factor. Therefore, to achieve optimal performance, both factors must be taken into account. Additionally, adjusting the variables mentioned earlier, i.e. VER, aeration capacity, and granule size can help balance treatment capacity and energy consumption for varying seasonal temperatures.

3.3. Perspectives

This study highlighted that explicit modelling of the dynamic behaviour of alpha can substantially improve the accuracy and reliability of predictions and advance our understanding of the AGS process. The performed trend analysis provided insights in the optimization of the design and operation of not only AGS processes but also other batch-wisely operated aerobic wastewater treatment systems. A 1-D AGS model including a dynamic aeration model and associated calibration procedure (Fig. S11 step 2 and 3) was described in detail to allow its further use by other researchers. While the model in this work was coded in Matlab-Simulink, many commercial simulators include pre-implemented granular sludge models which can also used for process optimization. The results in this work show that, independent of the model complexity and implementation, it is important to include the dynamics of alpha when describing the gas–liquid transfer.

The most important dynamic feature of alpha to be considered is its increase along the aeration phase. The results in this work were obtained with a dynamic aeration model including the relation between the alpha factor and the degradation of $bCOD_S$, considering the initial and final values of alpha previously determined for the plant under study. In order to generalize the applicability of the aeration model, the relation between alpha and $bCOD_S$ could be tested for varying influent conditions, which will further improve the knowledge on removal kinetics of different COD fractions. It is possible that the hydrolysis and fermentation processes in AGS systems which are now predicted by conventional equations and model parameters derived from activated sludge systems, such as ASM2d [36], needs to be recalibrated for the AGS process. Recent research has attempted to investigate hydrolysis in AGS batch reactors [52,53], but there is still limited information on the specific microorganisms involved and on the extent to which polymeric substrates contribute to anaerobic COD storage or aerobic and anoxic COD removal in AGS. Further research can help to develop an ASM matrix specific for AGS systems. Besides, the aeration model and thus optimization efforts could consider various other factors, such as the effect of reactor height, fouling, SRT, biomass concentration and rheology and soluble microbial metabolites on alpha dynamics [15].

Valuable insights were obtained regarding the qualitative influence of alpha dynamics on process performance under various operating strategies. It is important to note however that the results should not be interpreted in a fully quantitative way. The optimal setting of VER, aeration capacity and granule size, considering the prevailing temperature, will be case-specific. For instance, while this study focused on the removal of total nitrogen, in regions where the NH_4^+ effluent quality is the only parameter of concern, SND may be less relevant, changing the optimization strategy. For example, in the case of NH_4^+ limits only, it is preferable to select small granules and operate at a high aeration capacity to optimize OTE, reduce aeration costs and enhancing the nitrification rate. Conversely, in situations where energy is not limiting, the selection of large granules can significantly increase treatment capacity through SND, while meeting the total nitrogen criteria.

Finally, the proposed optimization strategies require full-scale validation to evaluate their economic feasibility and long-term impact on the system. Such full-scale validation would also help to clarify the impact of these strategies on energy consumption, an issue of growing importance.

4. Conclusions

This study demonstrated that the dynamic nature of the alpha factor affects the performance of a batch-wisely operated aerobic granular sludge (AGS) reactor. It was also shown that, in order to model the observed behaviour, specific considerations regarding the model structure apply.

The dynamic nature of alpha influences both the energy consumption and the treatment capacity. The energy consumption is influenced through dynamics in oxygen transfer efficiency, while the treatment capacity is influenced through the dynamics in simultaneous nitrification and denitrification. As a result, a dynamic alpha model is an essential part of mathematical models aiming to optimise the AGS process performance. Taking into account the dynamic nature of alpha in models instead of assuming a constant maximum alpha is essential to describe the observed relatively lower oxygenation capacity of the system at the start of the aeration.

The empirical relation between alpha and the removal of soluble biodegradable organic carbon ($bCOD_S$) can be adequately modelled by the extension of the biokinetic ASM2d model with a state variable S_{CB}, representing the soluble slowly biodegradable organic carbon. This model extension was necessary to evaluate the impact of the alpha factor on the process performance for different operating strategies. The microbial distribution in the granule and in the floc fraction is influenced by the alpha dynamics. In models assuming a fixed average granule size, the latter influence can be taken into account by the incorporation of a species-specific wasting factor (φ_i).

The dynamic nature of alpha can be exploited to optimize the reactor performance, through various process variables such as volume exchange ratio, aeration capacity, granule size and reactor temperature. Incorporating the influence of alpha on these variables during design

and operation reveals an optimal configuration that increases treatment capacity and reduces energy consumption.

The practical and model-related insights from this study facilitate the optimization of not only AGS processes but also other batch-wisely operated aerobic wastewater treatment systems.

5. Funding sources

The doctoral research work of Laurence Strubbe has been financially supported by a Doctoral fellowship of the Research Foundation – Flanders (FWO PhD fellowship strategic basic research 1SC1220N).

CRediT authorship contribution statement

Laurence Strubbe: Conceptualization, Data curation, Formal analysis, Funding acquisition, Investigation, Methodology, Software, Validation, Visualization, Writing – original draft. **Edward J.H. van Dijk:** Conceptualization, Supervision, Writing – review & editing. **Paula Carrera:** Conceptualization, Writing – review & editing. **Mark C.M. van Loosdrecht:** Conceptualization, Writing – review & editing. **Eveline I. P. Volcke:** Conceptualization, Project administration, Resources, Supervision, Writing – review & editing.

Declaration of competing interest

The authors declare that they have no known competing financial interests or personal relationships that could have appeared to influence the work reported in this paper.

Data availability

The data that has been used can be found in Supplemenatry Information.

Acknowledgements

We are grateful to Royal HaskoningDHV for the collaboration and for sharing the data. We also thank Prof. Krist V. Gernaey and Dr. Xavier Flores-Alsina of the Technical University of Denmark to provide us the Matlab-Simulink code of dr. Anna Katrine Vangsgaard which served as a basis for the development of the 1-D biofilm reactor model of this study.

Appendix A. Supplementary data

Supplementary data to this article can be found online at https://doi.org/10.1016/j.cej.2024.148843.

References

[1] M. Pronk, M.K. de Kreuk, B. de Bruin, P. Kamminga, R. Kleerebezem, M.C.M. van Loosdrecht, Full scale performance of the aerobic granular sludge process for sewage treatment, Water Res. 84 (2015) 207–217.https://doi.org/10.1016/j.watres.2015.07.011.

[2] A.C. van Haandel, J.G.M. van der Lubbe, Handbook of Biological Wastewater Treatment: Design and Optimisation of Activated Sludge Systems, IWA Publishing, 2012. ISBN (electronic): 9781780400808, https://doi.org/10.2166/9781780400808.

[3] E. Isanta, M. Figueroa, A. Mosquera-Corral, L. Campos, J. Carrera, J. Pérez, A novel control strategy for enhancing biological N-removal in a granular sequencing batch reactor: A model-based study, Chem. Eng. J. 232 (2013) 468–477, https://doi.org/10.1016/j.cej.2013.07.118.

[4] M. Layer, M.G. Villodres, A. Hernandez, E. Reynaert, E. Morgenroth, N. Derlon, Limited simultaneous nitrification-denitrification (SND) in aerobic granular sludge systems treating municipal wastewater: Mechanisms and practical implications, Water Res x. 7 (2020) 100048, https://doi.org/10.1016/J.WROA.2020.100048.

[5] S. Lochmatter, G. Gonzalez-Gil, C. Holliger, Optimized aeration strategies for nitrogen and phosphorus removal with aerobic granular sludge, Water Res. 47 (2013) 6187–6197, https://doi.org/10.1016/j.watres.2013.07.030.

[6] S. Lochmatter, J. Maillard, C. Holliger, Nitrogen removal over nitrite by aeration control in aerobic granular sludge sequencing batch reactors, Int J Environ Res Public Health. 11 (2014) 6955–6978, https://doi.org/10.3390/ijerph110706955.

[7] F. Sun, Y. Lu, J. Wu, Comparison of operational strategies for nitrogen removal in aerobic granule sludge sequential batch reactor (AGS-SBR): A model-based evaluation, J Environ Chem Eng. 7 (2019) 103314, https://doi.org/10.1016/J.JECE.2019.103314.

[8] J. Xu, H. Ju, J. He, H. Pang, The Performance of Aerobic Granular Sludge Under Different Aeration Strategies at Low Temperature, Water Air Soil Pollut. 233 (2022), https://doi.org/10.1007/S11270-022-05506-Y.

[9] Y. Kagawa, J. Tahata, N. Kishida, S. Matsumoto, C. Picioreanu, M.C.M. van Loosdrecht, S. Tsuneda, Modeling the nutrient removal process in aerobic granular sludge system by coupling the reactor- and granule-scale models, Biotechnol Bioeng. 112 (2015) 53–64, https://doi.org/10.1002/bit.25331.

[10] F. De Vleeschauwer, M. Caluwé, T. Dobbeleers, H. Stes, L. Dockx, F. Kiekens, C. Copot, J. Dries, A dynamic control system for aerobic granular sludge reactors treating high COD/P wastewater, using pH and DO sensors, J. Water Process Eng. 33 (2020) 101065, https://doi.org/10.1016/j.jwpe.2019.101065.

[11] N. Derlon, M.G. Villodres, R. Kovács, A. Brison, M. Layer, I. Takács, E. Morgenroth, Modelling of aerobic granular sludge reactors: the importance of hydrodynamic regimes, selective sludge removal and gradients, Water Sci. Technol. 86 (2022) 410–431, https://doi.org/10.2166/WST.2022.220.

[12] T. Dobbeleers, J. D'aes, S. Miele, M. Caluwé, V. Akkermans, D. Daens, L. Geuens, J. Dries, Aeration control strategies to stimulate simultaneous nitrification-denitrification via nitrite during the formation of aerobic granular sludge, Appl Microbiol Biotechnol. 101 (2017) 6829–6839, https://doi.org/10.1007/s00253-017-8415-1.

[13] E.J.H. van Dijk, K.M. Van Schagen, A.T. Oosterhoff, Controlled simultaneous nitrification and denitrification in wastewater treatment, 2018. Patent number: NL2018967B1.

[14] M.K. De Kreuk, J.J. Heijnen, M.C.M. Van Loosdrecht, Simultaneous COD, nitrogen, and phosphate removal by aerobic granular sludge, Biotechnol Bioeng. 90 (2005) 761–769, https://doi.org/10.1002/bit.20470.

[15] L. Strubbe, E.J.H. van Dijk, P.J.M. Deenekamp, M.C.M. van Loosdrecht, E.I. P. Volcke, Oxygen transfer efficiency in an aerobic granular sludge reactor: Dynamics and influencing factors of alpha, Chem. Eng. J. 452 (2023) 139548, https://doi.org/10.1016/J.CEJ.2022.139548.

[16] J.E. Baeten, E.J.H. van Dijk, M. Pronk, M.C.M. van Loosdrecht, E.I.P. Volcke, Potential of off-gas analyses for sequentially operated reactors demonstrated on full-scale aerobic granular sludge technology, Sci. Total Environ. 787 (2021) 147651, https://doi.org/10.1016/J.SCITOTENV.2021.147651.

[17] F. Cecconi, M. Garrido-Baserba, R. Eschborn, J. Damerel, D. Rosso, Oxygen transfer investigations in an aerobic granular sludge reactor, Environ Sci (camb). 6 (2020) 679–690, https://doi.org/10.1039/c9ew00784a.

[18] J. Alex, N.C. Holm, S.G.E. Rönner-Holm, Lag phase, dynamic alpha factor and ammonium adsorption behaviour: introduction of special activated sludge characteristics in the ASM3 + EAWAG-BioP-model, Water Sci Technol. 59 (2009) 133–140, https://doi.org/10.2166/WST.2009.588.

[19] S.G.E. Rönner-Holm, A. Mennerich, N.C. Holm, Specific SBR population behaviour as revealed by comparative dynamic simulation analysis of three full-scale municipal SBR wastewater treatment plants, Water Sci. Technol. 54 (2006) 71–80, https://doi.org/10.2166/WST.2006.373.

[20] D. Bencsik, I. Takács, D. Rosso, Dynamic alpha factors: Prediction in time and evolution along reactors, Water Res. 216 (2022), https://doi.org/10.1016/J.WATRES.2022.118339.

[21] L.M. Jiang, M. Garrido-Baserba, D. Nolasco, A. Al-Omari, H. DeClippeleir, S. Murthy, D. Rosso, Modelling oxygen transfer using dynamic alpha factors, Water Res. (2017), https://doi.org/10.1016/j.watres.2017.07.032.

[22] D. Rosso, R. Iranpour, M.K. Stenstrom, Fifteen Years of Offgas Transfer Efficiency Measurements on Fine-Pore Aerators: Key Role of Sludge Age and Normalized Air Flux, Water Environ. Res 77 (2005) 266–273, https://doi.org/10.2175/106143005X41843.

[23] S. Gillot, A. Héduit, Prediction of alpha factor values for fine pore aeration systems, Water Sci. Technol. 57 (2008) 1265–1269, https://doi.org/10.2166/WST.2008.222.

[24] J. Henkel, P. Cornel, M. Wagner, Oxygen transfer in activated sludge – new insights and potentials for cost saving, Water Sci. Technol. 63 (2011) 3034–3038, https://doi.org/10.2166/WST.2011.607.

[25] A.S. Ahmed, A. Khalil, Y. Ito, M.C.M. van Loosdrecht, D. Santoro, D. Rosso, G. Nakhla, Dynamic impact of cellulose and readily biodegradable substrate on oxygen transfer efficiency in sequencing batch reactors, Water Res. 190 (2021) 116724, https://doi.org/10.1016/J.WATRES.2020.116724.

[26] M.S. Zaghloul, G. Achari, A review of mechanistic and data-driven models of aerobic granular sludge, J Environ Chem Eng. 10 (2022), https://doi.org/10.1016/J.JECE.2022.107500.

[27] P.J. Roeleveld, M.C.M. Van Loosdrecht, Experience with guidelines for wastewater characterisation in The Netherlands, Water Sci. Technol. 45 (2002) 77–87, https://doi.org/10.2166/wst.2002.0095.

[28] J.P. Bassin, M. Pronk, R. Kraan, R. Kleerebezem, M.C.M. Van Loosdrecht, Ammonium adsorption in aerobic granular sludge, activated sludge and anammox granules, Water Res. 45 (2011) 5257–5265, https://doi.org/10.1016/J.WATRES.2011.07.034.

[29] P. Reichert, Aquasim - A tool for simulation and data analysis of aquatic systems, Water Sci. Technol. (1994), https://doi.org/10.2166/wst.1994.0025.

[30] J.E. Baeten, D.J. Batstone, O.J. Schraa, M.C.M. van Loosdrecht, E.I.P. Volcke, Modelling anaerobic, aerobic and partial nitritation-anammox granular sludge reactors - A review, Water Res. 149 (2019) 322–341, https://doi.org/10.1016/J.WATRES.2018.11.026.

[31] M.K. De Kreuk, C. Picioreanu, M. Hosseini, J.B. Xavier, M.C.M. Van Loosdrecht, Kinetic model of a granular sludge SBR: Influences on nutrient removal, Biotechnol Bioeng. 97 (2007) 801–815, https://doi.org/10.1002/bit.21196.
[32] E.J.H. van Dijk, V.A. Haaksman, M.C.M. van Loosdrecht, M. Pronk, On the mechanisms for aerobic granulation - model based evaluation, Water Res. 216 (2022) 118365, https://doi.org/10.1016/J.WATRES.2022.118365.
[33] A.K. Vangsgaard, Modeling, Experimentation, and Control of Autotrophic Nitrogen Removal in Granular Sludge Systems, Technical University of Denmark, Department of Chemical and Biochemical Engineering, 2013.
[34] A.K. Vangsgaard, M. Mauricio-Iglesias, K.V. Gernaey, B.F. Smets, G. Sin, Sensitivity analysis of autotrophic N removal by a granule based bioreactor: Influence of mass transfer versus microbial kinetics, Bioresour Technol. 123 (2012) 230–241, https://doi.org/10.1016/J.BIORTECH.2012.07.087.
[35] M. Kuśnierz, Scale of Small Particle Population in Activated Sludge Flocs, Water Air Soil Pollut. 229 (2018), https://doi.org/10.1007/S11270-018-3979-7.
[36] M. Henze, W. Gujer, T. Mino, M. van Loosdrecht, Activated Sludge Models ASM1, ASM2, ASM2d and ASM3 IWA Publishing. ISBN (electronic): 9781780402369, https://doi.org/10.2166/9781780402369.
[37] H. Hauduc, L. Rieger, I. Takács, A. Héduit, P.A. Vanrolleghem, S. Gillot, A systematic approach for model verification: Application on seven published activated sludge models, Water Sci. Technol. (2010), https://doi.org/10.2166/wst.2010.898.
[38] M.K.H. Winkler, R. Kleerebezem, L.M.M. De Bruin, P.J.T. Verheijen, B. Abbas, J. Habermacher, M.C.M. Van Loosdrecht, Microbial diversity differences within aerobic granular sludge and activated sludge flocs, Appl Microbiol Biotechnol. 97 (2013) 7447–7458, https://doi.org/10.1007/S00253-012-4472-7.
[39] E.I.P. Volcke, K. Solon, Y. Comeau, M. Henze, Chapter 3: Wastewater characteristics, in: G.H. Chen, M.C.M. van Loosdrecht, G.A. Ekama, D. Brdjanovic (Eds.), Biological Wastewater Treatment: Principles, Modeling and Design, IWA Publishing, 2020: pp. 77–110. https://doi.org/10.2166/9781789060362_0077.
[40] T. Nogaj, A. Randall, J. Jimenez, I. Takacs, C. Bott, M. Miller, S. Murthy, B. Wett, Modeling of organic substrate transformation in the high-rate activated sludge process, Water Sci. Technol. 71 (2015) 971–979, https://doi.org/10.2166/WST.2015.051.
[41] J.E. Baeten, M.C.M. van Loosdrecht, E.I.P. Volcke, Modelling aerobic granular sludge reactors through apparent half-saturation coefficients, Water Res. 146 (2018) 134–145, https://doi.org/10.1016/j.watres.2018.09.025.
[42] J.B. Xavier, M.K. De Kreuk, C. Picioreanu, M.C.M. Van Loosdrecht, Multi-scale individual-based model of microbial and byconversion dynamics in aerobic granular sludge, Environ Sci Technol. 41 (2007) 6410–6417, https://doi.org/10.1021/ES070264M/SUPPL_FILE/ES070264MSI20070705_065534.PDF.
[43] J.J. Beun, J.J. Heijnen, M.C.M. van Loosdrecht, N-removal in a granular sludge sequencing batch airlift reactor, Biotechnol Bioeng. 75 (2001) 82–92, https://doi.org/10.1002/BIT.1167.
[44] M. Ali, Z. Wang, K.W. Salam, A. Rao Hari, M. Pronk, M.C.M. van Loosdrecht, P. E. Saikaly, Importance of Species Sorting and Immigration on the Bacterial Assembly of Different-Sized Aggregates in a Full-Scale Aerobic Granular Sludge Plant, Environ. Sci. Technol. 53 (2019) 29, https://doi.org/10.1021/acs.est.8b07303.
[45] B. Nguyen Quoc, S. Wei, M. Armenta, R. Bucher, P. Sukapanpotharam, D.A. Stahl, H.D. Stensel, M.K.H. Winkler, Aerobic granular sludge: Impact of size distribution on nitrification capacity, Water Res. 188 (2021) 116445, https://doi.org/10.1016/J.WATRES.2020.116445.
[46] B. Nguyen Quoc, M. Armenta, J.A. Carter, R. Bucher, P. Sukapanpotharam, S. J. Bryson, D.A. Stahl, H.D. Stensel, M.K.H. Winkler, An investigation into the optimal granular sludge size for simultaneous nitrogen and phosphate removal, Water Res. 198 (2021), https://doi.org/10.1016/J.WATRES.2021.117119.
[47] M. Pronk, E.J.H. van Dijk, M.C.M. van Loosdrecht, Aerobic granular sludge, in: G. Chen, G.A. Ekama, M.C.M. van Loosdrecht, D. Brdjanovic (Eds.), Biological Wastewater Treatment: Principles, Modeling and Design, IWA Publishing, 2020: pp. 497–522. https://doi.org/10.2166/9781789060362_0497.
[48] D. Rosso, Aeration, Mixing, and Energy: Bubbles and Sparks, IWA Publishing, 2018. ISBN (electronic): 9781780407845, https://doi.org/10.2166/9781780407845.
[49] F. yuan Chen, Y.Q. Liu, J.H. Tay, P. Ning,, Operational strategies for nitrogen removal in granular sequencing batch reactor, J Hazard Mater. 189 (2011) 342–348, https://doi.org/10.1016/J.JHAZMAT.2011.02.041.
[50] Y. Li, Y. Liu, L. Shen, F. Chen, DO diffusion profile in aerobic granule and its microbiological implications, Enzyme Microb Technol. 43 (2008) 349–354, https://doi.org/10.1016/J.ENZMICTEC.2008.04.005.
[51] M.K. De Kreuk, M. Pronk, M.C.M. Van Loosdrecht, Formation of aerobic granules and conversion processes in an aerobic granular sludge reactor at moderate and low temperatures, Water Res. (2005), https://doi.org/10.1016/j.watres.2005.08.031.
[52] S. Toja Ortega, M. Pronk, M.K. de Kreuk, Anaerobic hydrolysis of complex substrates in full-scale aerobic granular sludge: enzymatic activity determined in different sludge fractions, Appl Microbiol Biotechnol. 105 (2021) 6073–6086, https://doi.org/10.1007/S00253-021-11443-3/FIGURES/5.
[53] S. Toja Ortega, L. van den Berg, M. Pronk, M.K. de Kreuk, Hydrolysis capacity of different sized granules in a full-scale aerobic granular sludge (AGS) reactor, Water Res x. 16 (2022), https://doi.org/10.1016/j.wroa.2022.100151.